nature geoscience

ARTICLES

PUBLISHED ONLINE: 17 APRIL 2017 | DOI: 10.1038/NGEO2932

River piracy and drainage basin reorganization led by climate-driven glacier retreat

Daniel H. Shugar[1]*, John J. Clague[2], James L. Best[3], Christian Schoof[4], Michael J. Willis[5], Luke Copland[6] and Gerard H. Roe[7]

River piracy—the diversion of the headwaters of one stream into another one—can dramatically change the routing of water and sediment, with a profound effect on landscape evolution. Stream piracy has been investigated in glacial environments, but so far it has mainly been studied over Quaternary or longer timescales. Here we document how retreat of Kaskawulsh Glacier—one of Canada's largest glaciers—abruptly and radically altered the regional drainage pattern in spring 2016. We use a combination of hydrological measurements and drone-generated digital elevation models to show that in late May 2016, meltwater from the glacier was re-routed from discharge in a northward direction into the Bering Sea, to southward into the Pacific Ocean. Based on satellite image analysis and a signal-to-noise ratio as a metric of glacier retreat, we conclude that this instance of river piracy was due to post-industrial climate change. Rapid regional drainage reorganizations of this type can have profound downstream impacts on ecosystems, sediment and carbon budgets, and downstream communities that rely on a stable and sustained discharge. We suggest that the planforms of Slims and Kaskawulsh rivers will adjust in response to altered flows, and the future Kaskawulsh watershed will extend into the now-abandoned headwaters of Slims River and eventually capture the Kluane Lake drainage.

River piracy, the diversion of the headwaters of one stream into another with a higher gradient[1], can alter the location of a drainage divide and dramatically change the routing of water and sediment, with a profound effect on landscape evolution[2–4]. Although some researchers have examined stream piracy in glacial environments[5–7], relatively little attention has been given to proglacial drainage changes. Furthermore, previous studies of river piracy have dealt with capture over Quaternary or longer timescales, with no one, to our knowledge, having detailed the phenomenon in the modern era. Herein, we document rapid river piracy at the front of Kaskawulsh Glacier, Yukon (Fig. 1), which occurred in May 2016.

The toe of Kaskawulsh Glacier lies at a drainage divide that separates the Alsek River watershed, which drains to the North Pacific Ocean, from the Yukon River watershed, which drains to the Bering Sea. Prior to May 2016, some of the water flowing from the toe of the glacier marked the headwaters of Kaskawulsh River, a major tributary of Alsek River. The remainder of the water issuing from the glacier flowed via Slims River into Kluane Lake, the largest lake in Yukon and part of the Yukon River watershed. Ongoing thinning and retreat of the glacier, caused by over a century of climate warming[8–12], triggered the river piracy, which was geologically instantaneous and is likely to be permanent. Substantial long-term hydrological and ecological impacts[13,14] may be expected as a result, including a reversal in outflow from Kluane Lake, diminished outflow at the north end of the lake, and perhaps even seasonal closure of the lake basin.

Recent history of Kaskawulsh Glacier and its terminal lakes

In the early Holocene, when the climate of southwest Yukon was warmer than today, Kluane Lake discharged to the south towards the Alsek River[15]. Kaskawulsh Glacier achieved its maximum extent between ~1717 and the mid-1750s[16–18]. During this Little Ice Age advance, sediment from the glacier deposited an outwash fan, which raised the base level of a river that formerly drained south from Kluane Lake (Fig. 1), perhaps through much of the Holocene[19]. By the middle of the eighteenth century, the glacier completely blocked this south-flowing river, initiating the north-flowing Slims River, which rapidly built a delta and floodplain into Kluane Lake. The lake rose about 12 m above the 2006 datum and flowed over a debris fan at the north end of the lake, rapidly returning the lake to its present level[15,19]. Kaskawulsh Glacier began to retreat in the nineteenth century, with retreat accelerating in the late twentieth and early twenty-first centuries. Between 1956 and 2007, for example, the glacier retreated 655 m (ref. 9). Roe *et al.*[12] recently developed a method to test a glacier's retreat against the null hypothesis that retreat was due to natural climate variability. Applying this analysis to the Kaskawulsh Glacier (see Methods and Supplementary Fig. 1), we find there is only a 0.5% chance that retreat over the past century—and by extension, the observed piracy—could have happened under a constant climate. We therefore conclude that retreat of Kaskawulsh Glacier is attributable to observed warming over the industrial era.

Recent retreat of Kaskawulsh Glacier has been accompanied by the growth of terminal lakes, the largest of which we name

[1]Water, Sediment, Hazards and Earth-surface Dynamics (WaterSHED) Lab, School of Interdisciplinary Arts and Sciences, University of Washington Tacoma, Tacoma, Washington 98402, USA. [2]Centre for Natural Hazards Research, Department of Earth Sciences, Simon Fraser University, Burnaby, British Columbia V5A 1S6, Canada. [3]Departments of Geology, Geography and GIS, Mechanical Science and Engineering and Ven Te Chow Hydrosystems Laboratory, University of Illinois, Urbana, Illinois 61801, USA. [4]Department of Earth, Ocean & Atmospheric Sciences, University of British Columbia, Vancouver, British Columbia V6T 1Z4, Canada. [5]Cooperative Institute for Research in Environmental Sciences, University of Colorado, Boulder, Colorado 80309, USA. [6]Department of Geography, Environment and Geomatics, University of Ottawa, Ottawa, Ontario K1N 6N5, Canada. [7]Department of Earth and Space Sciences, University of Washington, Seattle, Washington 98195, USA. *e-mail: dshugar@uw.edu

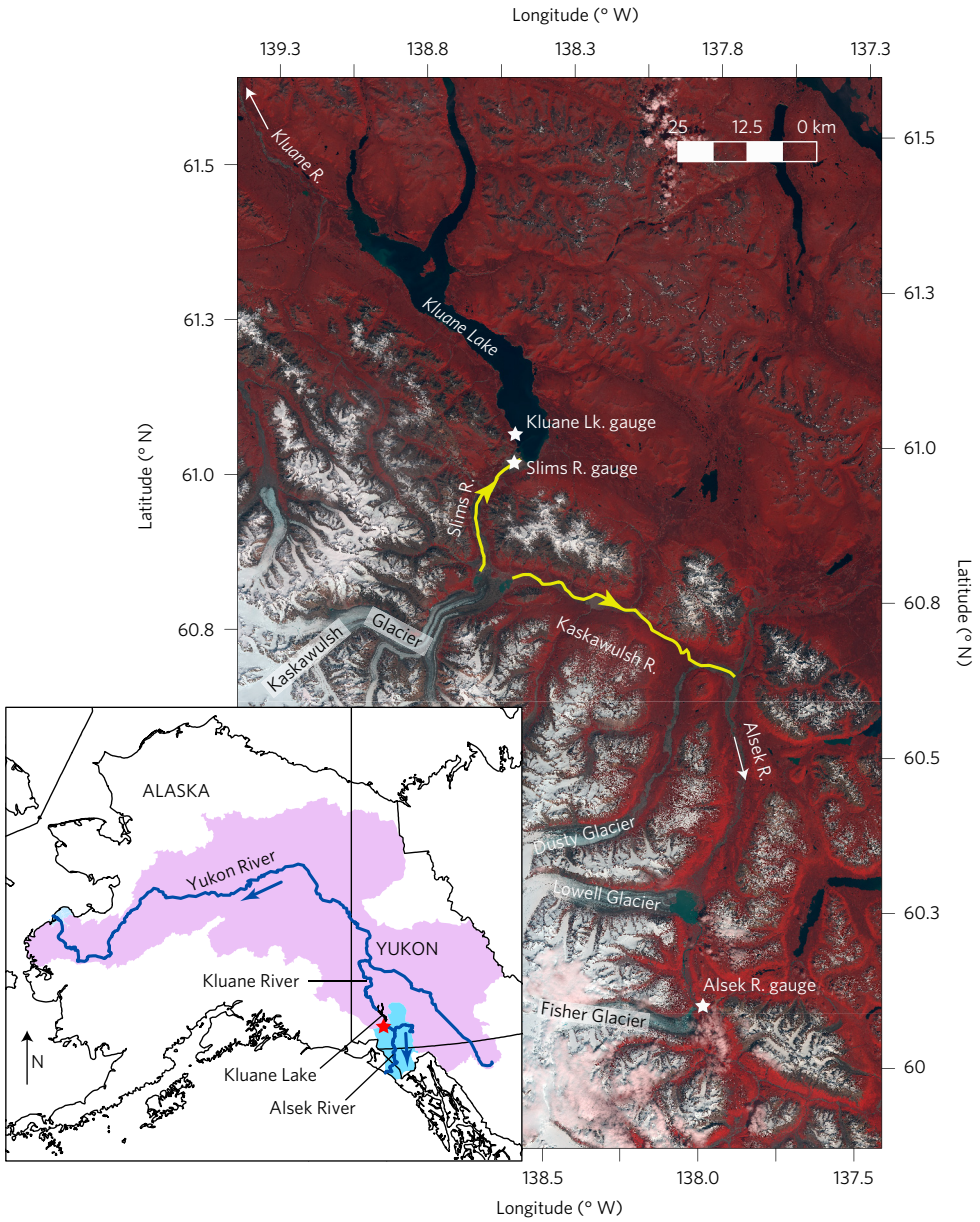

Figure 1 | Satellite image showing the Slims, Kaskawulsh and upper Alsek rivers, and Kluane Lake. Locations of river and lake gauges are shown with white stars. Yellow lines with arrows represent pre-2016 flow paths of the Slims and Kaskawulsh rivers. Inset map of Alaska and Yukon shows the Yukon (pink shading) and Alsek (blue shading) watersheds. Red star indicates study area at the south end of Kluane Lake.

'Slims Lake' and 'Kaskawulsh Lake' (Fig. 2). Outflow from Slims Lake has historically been northward into Kluane Lake via Slims River, whereas outflow from Kaskawulsh Lake has historically been southward to Alsek River via Kaskawulsh River (Fig. 1). A 1956 aerial photograph[9] shows a small Slims Lake on the west side of the glacier terminus. Only isolated ponds are visible in 1972 and 1980, with no lake at all in 1990 (Fig. 2). However, by 2000, Slims Lake had grown to 1.1×10^6 m^2, and by 2015 its area had increased more than threefold to 3.9×10^6 m^2 (Fig. 2b,h). By August 2016 (Fig. 2b,i), Slims Lake had partially drained, its area decreasing to 1.0×10^6 m^2, stranding the outlet of Slims River ~17 m above the level of the remnant water body.

The earliest Landsat scene (2 September 1972) shows a small (~1.1×10^6 m^2) Kaskawulsh Lake at the east margin of the glacier terminus (Fig. 2). The lake expanded to ~1.9×10^6 m^2 by 2010, and to ~2.7×10^6 m^2 by 2015. By early July 2016, its size was three times that in 1982 (~3.3×10^6 m^2).

Drainage reorganization in 2016

Although the Slims River gauge record has gaps (Fig. 3g), a clear reduction in river level is apparent in May 2016. Normal diurnal fluctuations ended with an abrupt four-day drop in river level commencing on 26 May 2016. Over the remainder of the summer of 2016, the level of Slims River was 0.7–1.0 m below the average for those days. Our acoustic Doppler current profiler measurements at the Slims River bridge on 3 September 2016, indicated a discharge of ~11 m^3 s^{-1}, less than that reported following the 1970 (~21 m^3 s^{-1}) diversion. Although we have no measurements immediately prior to the 2016 piracy, pre-diversion flows of ~130 m^3 s^{-1} have been reported for 1970[20].

The reduction of Slims River flow has had substantial effects at Kluane Lake. The lake had a record minimum water level in early May 2016 (Fig. 3a–c), about 0.1 m below its previously recorded low in May 2015. By the time of its normal seasonal peak (early August), the lake was ~1.7 m below its long-term mean level and 1 m below

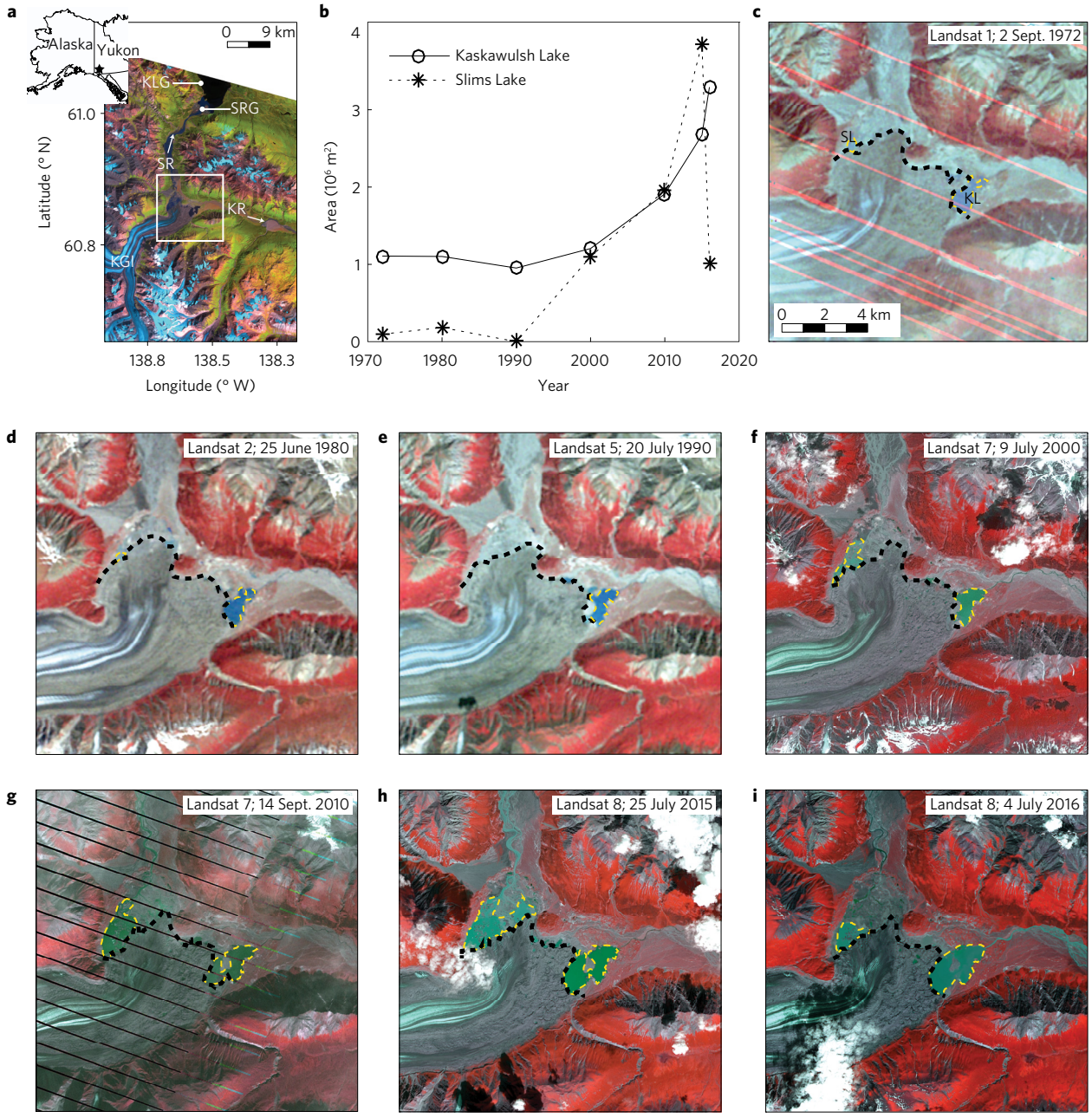

Figure 2 | Time series of Kaskawulsh Glacier terminus and lake extents. a, Map of southwest Yukon showing the location of Kluane Lake (SPOT-5 08-14-15). Kaskawulsh Glacier (1,053 km^2), one of the main outlet glaciers of the St Elias Icefield, the largest non-polar icefield in the world[28], flows ~80 km east from the St Elias Mountains and terminates at a drainage divide. The white box in **a** shows the area of the satellite images in **c**–**i**. **b**, Changes in the areal extent of lakes at the terminus of Kaskawulsh Glacier from 1972 to 2016. **c**–**i**. Landsat images showing changes to the terminus of Kaskawulsh Glacier and its proglacial lakes on an approximately decadal timescale. KR, Kaskawulsh River; SR, Slims River; KLG, Kluane Lake gauge; SRG, Slims River gauge; KGI, Kaskawulsh Glacier; SL, Slims Lake; KL, Kaskawulsh Lake. Dashed yellow lines in **c**–**i** indicate extents of the two lakes. Dashed black lines delineate glacier terminus.

its lowest recorded level for that time of year. The lowering of Kluane Lake in 2016 equates to a volumetric reduction of ~0.67 km^3 relative to the historic average.

Alsek River discharge (Fig. 3d–f) fluctuated around the historic mean until early July 2016, after which it rose sharply and fluctuated around the historic maximum level for that time of year, at times exceeding it by ~1 m. The peak discharge in 2016 occurred on 20 July (1,470 m^3 s^{-1}), which is nearly as high as any previously recorded peak flow (1,550 m^3 s^{-1}, 13 July, 1989) and 87% higher than the average peak discharge during the 41-yr period of record (783 m^3 s^{-1}). The elevated discharge was probably the result of the emptying of the eastern part of Slims Lake and lowering of its western part, with the consequent re-routing of water from Slims River into Kaskawulsh River. By October 2016, Alsek River discharge had dropped to its historic mean, reflecting the reduction in discharge from glacier melt at the end of the summer.

About 15 mm of rain fell at Haines Junction on 2 May 2016, but there was little other precipitation during the first half of 2016 (Supplementary Fig. 2). It is therefore unlikely that rainfall contributed significantly to the mid-summer increase in Alsek River discharge. Meteorological records from Haines Junction and the Kaskawulsh Glacier nunatak indicate that mean daily temperatures

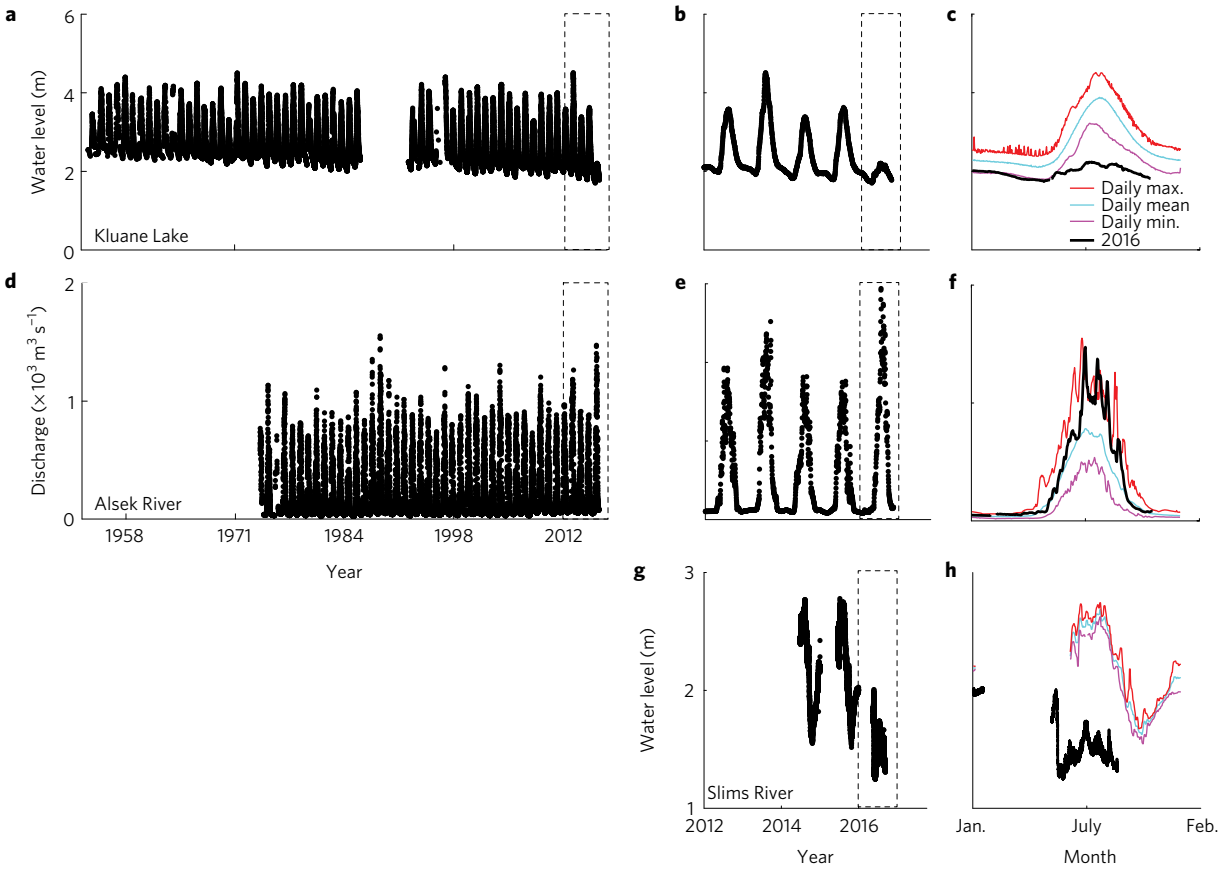

Figure 3 | Hydrographs for Kluane Lake, Alsek River and Slims River for the period 1952–2016. a,**d**,**g**, Entire record for each station (dashed rectangles are enlarged in **b**,**e**,**h**). **c**,**f**,**h**, Daily minimum, mean and maximum monthly values averaged over the full data period excluding 2016; 2016 data are shown in black. Data for Kluane Lake (gauge 09ca001) and Alsek River (08ab001) are from Environment Canada. The Alsek River gauge is located ~110 km downstream of the terminus of Kaskawulsh Glacier (Fig. 1). Its largest single source of water is Kaskawulsh River. The water-level record at Kluane Lake (**a**) shows a gradual long-term decrease, most notably in the seasonal low water level. It is unclear whether this gradual lowering reflects reduced inputs from Slims River, or perhaps greater outflow from Kluane River as a result of channel widening or deepening.

during the period January–April 2016 were, respectively, 4.3 °C and 3.6 °C warmer than the 2007–2016 decadal means for the same three-month period (Supplementary Fig. 2), which itself was probably the warmest decade of the past century[21]. At Haines Junction, which is 300 m lower than the glacier terminus, mean daily temperatures were above freezing almost continuously after mid-March, approximately one month earlier than the decadal mean. At the nunatak, which is 1,000 m higher than the terminus, the main period of above-freezing conditions started in early May, ~1.5 weeks earlier than normal, and air temperatures were unusually warm immediately before the drop in the level of Slims River (Supplementary Fig. 2). It thus seems likely that Kaskawulsh Glacier experienced unusually high surface melt in the spring of 2016, which lead to development of an ice-walled canyon (Fig. 4 and Supplementary Fig. 3) and increased flow in Kaskawulsh and Alsek rivers.

The ice-walled channel that was established across dead ice at the terminus of Kaskawulsh Glacier (Fig. 4 and Supplementary Fig. 3) was rapidly enlarged by meltwater and localized collapse of the channel walls in the summer of 2016, resulting in the 17 m lowering of Slims Lake. Even if the current canyon walls were to collapse and temporarily block the flow of meltwater into Kaskawulsh Lake, the blockage could not pond water in Slims Lake to the level required to re-establish Slims River. For example, at transect A–A′ near the upstream end of the canyon (Fig. 4), the channel floor is at ~785 m a.s.l. For an ice blockage to raise water levels to reconnect to Slims River (head at 805 m a.s.l.), Slims Lake would need to be >20 m deep, which is more than the height of the canyon walls (Fig. 4b). Only a re-advance of Kaskawulsh Glacier could block the channel and refill Slims Lake, but this is very unlikely given recent and current climate trends. We therefore conclude that the drainage change is permanent.

Previous workers[19] had predicted the capture of Slims River by Kaskawulsh River, although they were unable to predict when, or how rapidly, that change might happen. These predictions were based, in part, on the fact that Kaskawulsh River has a much steeper gradient than Slims River—the uppermost reach of Kaskawulsh River has a gradient of 6.1 m km^{-1}, almost five times that of upper Slims River (1.3 m km^{-1}, Fig. 5). Furthermore, the surface of Kaskawulsh Lake is approximately 50 m lower than that of Slims Lake (755 m versus 805 m a.s.l. in September 2016), and also approximately 25 m lower than that of Kluane Lake (~780 m a.s.l. in September 2016).

Implications of drainage reorganization

The piracy of Slims River has five important downstream implications. First, the level of Kluane Lake has fallen and may fall further, potentially below its outlet at the north end of the lake (Fig. 1). If this happens, Kluane Lake will become a closed basin. Second, the large supply of sediment to Kluane Lake from Slims River[22–24] has ended, with unknown effects on the structure and chemistry of the lake and its ecosystems[25]. For example, in summer 2016, massive afternoon dust storms occurred almost daily on the nearly abandoned Slims River floodplain (Supplementary

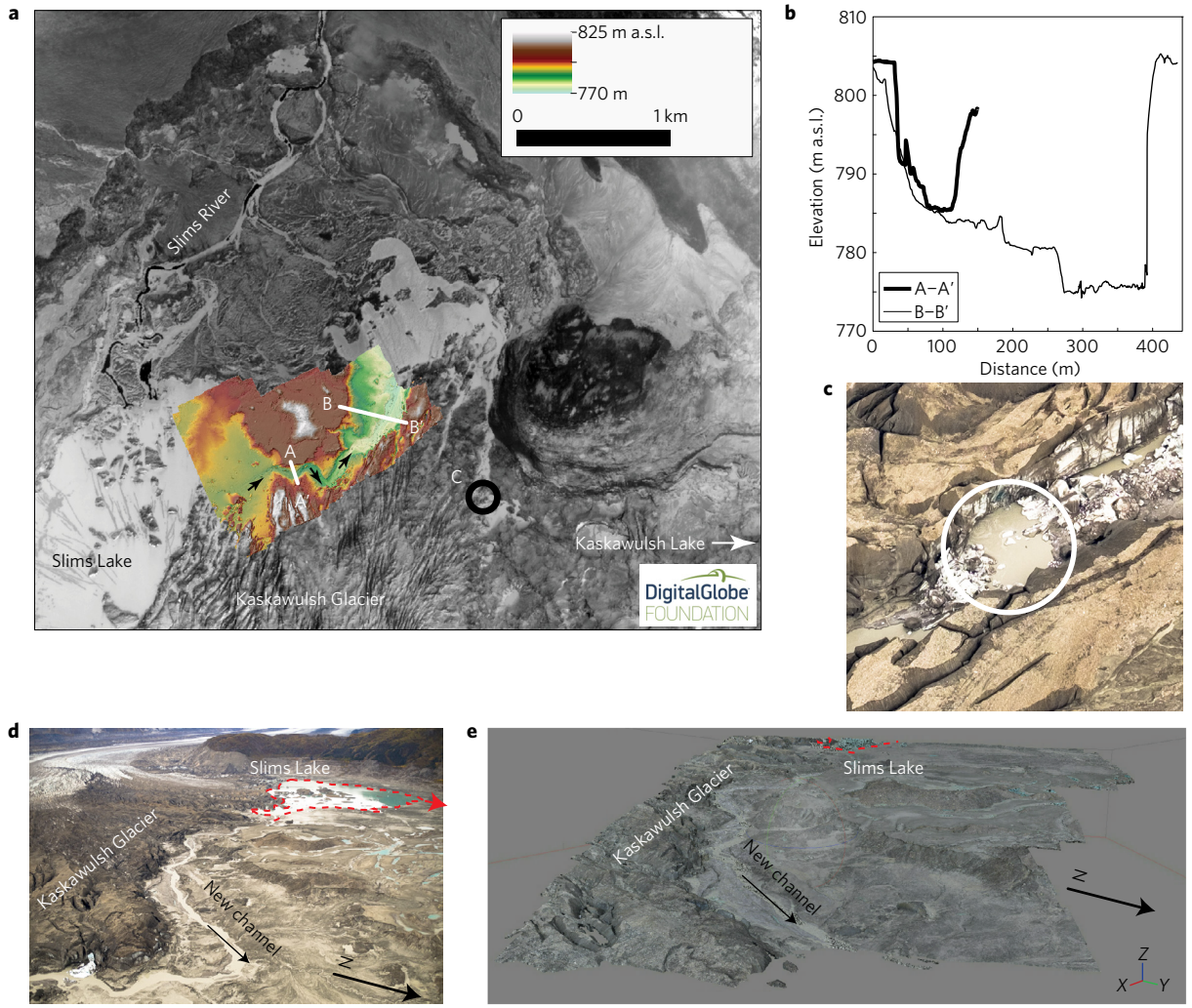

Figure 4 | Drone-generated digital elevation model (DEM), topographic profiles and photographs of the terminus of Kaskawulsh Glacier and its proglacial lakes in September 2016. a–c, High-resolution (0.25 m) drone-generated DEM overlain on orthorectified panchromatic WorldView-1 scene from 29 October 2012. Satellite image courtesy of the DigitalGlobe Foundation, 2012. Note that the proglacial lakes are frozen in this early winter image. The 5.7-km-long channel ranged in width from ~20 m to ~100 m and was up to ~20 m deep. At the time of our survey on 2 September 2016, the river at the bottom of the canyon was ~20 m wide (Supplementary Fig. 3) and was being fed partly by a subglacial channel ~2.7 km downstream of the head of the river. Black arrows in **a** indicate the flow path through the ice-walled canyon. Profiles A–A′ and B–B′ are shown in **b**, and the black circle labeled 'c' indicates the location of the subglacial channel outflow shown in **c**. It is unclear if the location of this subglacial channel was the same before establishment of the canyon or facilitated its creation. **d**, Photograph (2 September 2016) of the Kaskawulsh Glacier terminus, Slims Lake (the former outlet feeding Slims River is shown by the red arrow), and the new channel linking Slims Lake and Kaskawulsh Lake. **e**, Drone-generated point cloud with the same perspective as in **d**, coloured with RGB values.

Fig. 3) due to the lower lake level, possibly altering nutrient fluxes to the lake. Third, Slims, Kaskawulsh and Alsek rivers must now all adjust to altered discharges. For example, as flow and sediment transport in Slims River have decreased greatly, channel stability there may increase, resulting in conversion from a braided to a wandering or meandering river planform[26]. Increased flows in Kaskawulsh River may increase sediment conveyance and bank erosion. Fourth, large-scale changes to drainage basin geometry and re-routing of meltwater may introduce considerable changes to fish populations and habitat, including effects produced by the timing of flows[27]. Fifth, assuming that Kaskawulsh Glacier continues to thin and recede, Kaskawulsh River may advance its drainage headward (northward) into the easily erodible Slims River valley fill and towards Kluane Lake, thereby capturing the discharge of the small mountain streams that previously joined Slims River. It is noteworthy that the present head of Kaskawulsh River is ~25 m below the current level of Kluane Lake and, as a consequence, there is gravitational potential to drive continued expansion of the Kaskawulsh River catchment towards the lake (Fig. 5). Thus, over time, headward erosion could result in Kaskawulsh River reaching the south end of Kluane Lake and re-establishing its former southerly drainage to the Pacific Ocean[15,19].

These effects highlight the consequences of climate-induced glacier retreat, and river piracy triggered by such retreat, on the routing of water and sediment across a deglaciating landscape. Such changes undoubtedly were common, and probably occurred on a larger scale, during the decay of ice sheets in North America and Eurasia at the close of the Pleistocene, as shown by abandoned and buried valleys that are common features of formerly glaciated landscapes. We contend that radical reorganizations of drainage can occur in a geologic instant, although they may also be driven by longer-term climate change. The potential consequences of such channel re-routing and environmental change are amplified by anthropogenic activity and settlement, and these effects can be

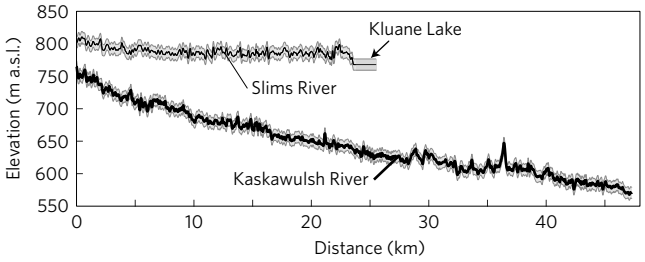

Figure 5 | Longitudinal profiles of the Slims and Kaskawulsh rivers. Elevations are derived from the 30-m ASTER GDEM v2 and smoothed using a 5-bin moving average filter. The grey error envelope represents the published root mean square error (RMSE) of ~8.7 m (ref. 29). The absolute vertical accuracy is 17 m. Profile locations are shown as solid yellow lines in Fig. 1.

expected to have significant effects on both ecosystem functioning and economic infrastructure, for example hydroelectric power generation and water supply, as glacier retreat proceeds in a future warming climate. Most studies of the effects of climate change on glacial environments deal with enhanced melt or contributions to sea-level rise. We suggest that the effects can be more far reaching.

Methods

Methods, including statements of data availability and any associated accession codes and references, are available in the online version of this paper.

Received 5 December 2016; accepted 13 March 2017; published online 17 April 2017

References

1. Bates, R. L. & Jackson, J. A. Dictionary of geological terms. *Am. Geol. Inst.* 386 (1984).
2. Willett, S. D., McCoy, S. W., Perron, J. T., Goren, L. & Chen, C. Y. Dynamic reorganization of river basins. *Science* **343,** 1248765 (2014).
3. Bishop, P. Drainage rearrangement by river capture, beheading and diversion. *Prog. Phys. Geogr.* **19,** 449–473 (1995).
4. Vella, P., Neef, G. & Kaewyana, W. River piracy at Kakariki, north-western Wairarapa, New Zealand. *J. R. Soc. N.Z.* **17,** 373–380 (1987).
5. Carter, S. P., Fricker, H. A. & Siegfried, M. R. Evidence of rapid subglacial water piracy under Whillans Ice Stream, West Antarctica. *J. Glaciol.* **59,** 1147–1162 (2013).
6. Smith, L. C. *et al*. Efficient meltwater drainage through supraglacial streams and rivers on the southwest Greenland ice sheet. *Proc. Natl Acad. Sci. USA* **112,** 1001–1006 (2015).
7. Vaughan, D. G., Corr, H. F. J., Smith, A. M., Pritchard, H. D. & Shepherd, A. Flow-switching and water piracy between Rutford Ice Stream and Carlson Inlet, West Antarctica. *J. Glaciol.* **54,** 41–48 (2008).
8. Flowers, G. E., Copland, L. & Schoof, C. G. Contemporary glacier processes and global change: recent observations from Kaskawulsh Glacier and the Donjek Range, St. Elias Mountains. *Arctic* **67,** 22–34 (2014).
9. Foy, N., Copland, L., Zdanowicz, C., Demuth, M. & Hopkinson, C. Recent volume and area changes of Kaskawulsh Glacier, Yukon, Canada. *J. Glaciol.* **57,** 515–525 (2011).
10. Arendt, A. A., Echelmeyer, K. A., Harrison, W. D., Lingle, C. S. & Valentine, V. B. Rapid wastage of Alaska glaciers and their contribution to rising sea level. *Science* **297,** 382–386 (2002).
11. Berthier, E., Schiefer, E., Clarke, G. K. C., Menounos, B. & Remy, F. Contribution of Alaskan glaciers to sea-level rise derived from satellite imagery. *Nat. Geosci.* **3,** 92–95 (2010).
12. Roe, G. H., Baker, M. B. & Herla, F. Centennial glacier retreat as categorical evidence of regional climate change. *Nat. Geosci.* **10,** 95–99 (2017).
13. Fleming, S. W. Comparative analysis of glacial and nival streamflow regimes with implications for lotic habitat quantity and fish species richness. *River Res. Appl.* **21,** 363–379 (2005).
14. Franzin, W. G. & Clayton, J. W. A biochemical genetic study of zoogeography of lake whitefish (*Coregonus clupeaformis*) in western Canada. *J. Fish Res. Board Can.* **34,** 617–625 (1977).
15. Bostock, H. S. *Kluane Lake, Yukon Territory, Its Drainage and Allied Problems* 69–28 (Geological Survey of Canada Papers, 1969).
16. Borns, H. W. Jr & Goldthwait, R. P. in *Icefield Ranges Research Project, Scientific Results* Vol. 1 (eds Bushnell, V. C. & Ragle, R. H.) 187–196 (American Geographical Society, Arctic Institute of North America, 1969).
17. Denton, G. H. & Stuiver, M. Neoglacial chronology, northeastern St. Elias Mountains, Canada. *Am. J. Sci.* **264,** 577–599 (1966).
18. Reyes, A. V., Luckman, B. H., Smith, D. J., Clague, J. J. & Van Dorp, R. D. Tree-ring dates for the maximum Little Ice Age advance of Kaskawulsh Glacier, St. Elias Mountains, Canada. *Arctic* **59,** 14–20 (2006).
19. Clague, J. J. *et al*. Rapid changes in the level of Kluane Lake in Yukon Territory over the last millennium. *Quat. Res.* **66,** 342–355 (2006).
20. Bryan, M. L. Variations in quality and quantity of Slims River water, Yukon Territory. *Can. J. Earth Sci.* **9,** 1469–1478 (1972).
21. Wijngaarden, J. Temperature trends in the Canadian arctic during 1895–2014. *Theor. Appl. Clim.* **120,** 609–615 (2015).
22. Shugar, D. H. in *Yukon Exploration and Geology 2013* (eds MacFarlane, K. E., Nordling, M. G. & Sack, P. J.) 221–231 (Yukon Geological Survey, 2014).
23. Bryan, M. L. Sedimentation in Kluane Lake, Yukon Territory, Canada. *Proc. Assoc. Am. Geogr.* **2,** 31–35 (1970).
24. Crookshanks, S. *High-Energy Sedimentary Processes in Kluane Lake, Yukon Territory* MSc thesis, Queen's Univ. (2008).
25. Lister, G. S., Kelts, K., Zao, C. K., Yu, J.-Q. & Niessen, F. Lake Qinghai, China: closed basin lake levels and the oxygen isotope record for Ostracoda since the latest Pleistocene. *Palaeogeogr. Palaeoclimatol. Palaeoecol.* **84,** 141–162 (1991).
26. Church, M. Bed material transport and the morphology of alluvial river channels. *Ann. Rev. Earth Planet. Sci.* **34,** 325–354 (2006).
27. McParland, D., Eaton, B. & Rosenfeld, J. At-a-station hydraulic geometry simulator. *River Res. Appl.* **32,** 399–410 (2016).
28. Arendt, A. *et al*. Randolph Glacier Inventory—A Dataset of Global Glacier Outlines: Version 4.0.Boulder, CO: Global Land Ice Measurements from Space (2014).
29. Tachikawa, T. *et al*. *ASTER Global Digital Elevation Model Version 2—Summary of Validation Results* 26 (NASA, 2011).

Acknowledgements

We thank S. Williams and L. Goodwin for providing accommodation and meals at the Kluane Lake Research Station (Arctic Institute of North America field station). L. Goodwin and M. Schmidt (Arctic Institute of North America) provided useful insights and photographs from the spring of 2016, and N. Roberts, K. Kennedy, H. Rawley and P. Lipovsky assisted with fieldwork. TransNorth Helicopters flew us to and from the terminus of Kaskawulsh Glacier. Financial support for the fieldwork and data analysis was provided by Parks Canada, Yukon Geological Survey, University of Washington (Royalty Research Fund award A106655), Natural Sciences and Engineering Research Council of Canada (awards 24595, 342027-12, 346116-12, 357193-13, and 361960-13), University of Ottawa, Polar Continental Shelf Program, and the Jack and Richard Threet Chair in Sedimentary Geology at the University of Illinois. The DigitalGlobe Foundation and the European Space Agency's Spot-5 Take-5 programme provided high-resolution optical satellite data. We thank the University of North Carolina at Chapel Hill Research Computing group for providing computational resources that have contributed to these research results. Geospatial support for this work provided by the Polar Geospatial Center under NSF PLR awards 1043681 and 1559691. C. Zdanowicz and the Geological Survey of Canada supplied meteorological data for the Kaskawulsh Glacier. R. Watt and E. Higgs (Mountain Legacy Project) helped us acquire historical photographs. Permits from Parks Canada, and Yukon Territorial Government enabled the research, which was conducted on the traditional territory of the Kluane First Nation and Champagne-Aishihik First Nation. We are very grateful for the opportunity to accomplish this work.

Author contributions

D.H.S., J.J.C. and J.L.B. conceived the study and collected, processed and analysed field data. D.H.S. performed GIS and hydrological analyses. C.S. provided Slims River gauge data. L.C. provided and analysed meteorological data, as well as inputs for glacier retreat modelling. M.J.W. produced the high-resolution satellite DEM. G.H.R. contributed glacier retreat calculations. All authors contributed to writing and revising the paper.

Additional information

Supplementary information is available in the online version of the paper. Reprints and permissions information is available online at www.nature.com/reprints. Publisher's note: Springer Nature remains neutral with regard to jurisdictional claims in published maps and institutional affiliations. Correspondence and requests for materials should be addressed to D.H.S.

Competing financial interests

The authors declare no competing financial interests.

Methods

To provide insight into the evolution of regional drainage, we produced structure-from-motion digital elevation models (SfM DEM) of the proglacial environment of Kaskawulsh Glacier from drone (DJI Phantom 3 Pro) and helicopter imagery, using a Trimble R10 real-time kinematic Global Navigation Satellite System (RTK-GNSS) to establish ground control points and survey lake outlet elevations. We processed drone and helicopter photos to point clouds using Agisoft Photoscan and converted them to DEMs in ArcGIS 10.3. We were unable to estimate vertical errors by comparing the photo-based DEMs with other DEM sources, because the terrain over which the drone data were acquired changed over time. Instead, we conservatively estimate the error to be 1 m (ref. 30).

We compared high- and medium-resolution satellite (WorldView, SPOT-5, and Landsat) time series of the glacier terminus and digitized the extent of proglacial lakes from Landsat images acquired between 1972 and 2016 (Supplementary Table 1). A 2-m-resolution DEM derived from along-track stereo WorldView-1 imagery was constructed using the SETSM algorithm[31]. We used this DEM to calculate gradients for the uppermost 4 km of Slims and Kaskawulsh rivers. Topographic profiles of the entire length of each river were constructed from ASTER Global Digital Elevation Model (GDEM) v2 data. ASTER GDEM is a product of NASA and METI. The ASTER GDEM v2 has an RMSE of ∼8.7 m and an absolute vertical error of 17 m (ref. 29).

We examined gauge records for Slims River, Kaskawulsh River and Kluane Lake for the period of interest and collected discharge data for Slims River in September 2016, after the piracy event, using an acoustic Doppler current profiler (aDcp; 1,200 kHz Teledyne RiverPro) mounted on a tethered boat. An Environment Canada water-level gauge in Kluane Lake (#09ca001), near the mouth of Slims River (61° 03′ 16″ N, 138° 30′ 21″ W), has been operating since late 1952, with a data gap between 1987 and 1993. Another Environment Canada gauge on Alsek River (#08ab001; 60° 07′ 05″ N, 137° 58′ 39″ W), approximately 115 km downstream of Kaskawulsh Lake, has recorded discharge almost daily since 1974. Data from Slims River were obtained using a Campbell Scientific SR50 sonic ranger installed on the Slims River bridge at the south end of Kluane Lake (61° 00′ 04″ N, 138° 30′ 36″ W) in June 2014, with gaps during winter due to solar power outages. The SR50 sonic ranger measures distance to the water surface. We corrected temperature-induced differences in the speed of sound using an adjacent temperature sensor and then converted these distances to water depth by calculating the distance of the SR50 sensor to the riverbed. We summed the width-averaged water depths determined from an aDcp transect with an SR50 reading made at the same time and day. We assume that bed elevation did not change during the period of acquisition. This height was then differenced from the SR50 readings to the water surface to yield an estimate of water depth.

A meteorological station located on a nunatak between the north and central arms of Kaskawulsh Glacier (60° 44′ 32″ N, 139° 09′ 59″ W, 1,845 m a.s.l.), approximately 30 km upglacier (west–southwest) from the glacier terminus, provided air temperatures for the period 2007–2016. Temperatures were measured with a Campbell Scientific 107F temperature probe, with an accuracy of ±0.2 °C, and recorded hourly on a Campbell Scientific CR10x logger. We also acquired data from the Environment Canada meteorological station at Haines Junction (station ID 2100630, 60° 46′ 21″ N, 137° 34′ 49″ W, 595 m a.s.l.), approximately 55 km east of the terminus of Kaskawulsh Glacier. We used the daily mean, maximum, and minimum air temperatures at this station from 2007 to 2016, together with the total daily precipitation from January to June 2016.

We evaluated whether the retreat of Kaskawulsh Glacier might be due to natural variability using the method developed by Roe and colleagues[12]. The results are shown in Supplementary Fig. 1. The width-averaged retreat of Kaskawulsh Glacier between 1899 and 2016 was 1.9 km, based on an average of 13 distance measurements taken across the glacier terminus following the methodology of Foy and colleagues[9]. The 2016 terminus position was determined from a Landsat 8 image acquired on 8 October 2016. The position of the terminus in 1899 was recorded by a series of oblique photos taken by A.H. Brooks during a surveying expedition, which we acquired from the National Archives, Ottawa, Canada[32].

The method of Roe *et al.* is summarized as follows. Let ΔL be the change in glacier length over the past 130 years (∼1.9 km), and let σ_L be the standard deviation of glacier length due to stochastic fluctuations in mass balance, b, from natural, interannual climate variability. The signal-to-noise ratio is defined by $s_L = \Delta L/\sigma_L$. Likewise, $s_b = \Delta b/\sigma_b$. Ref. 12 demonstrates that the two are related via $s_L = \gamma s_b$, where γ is an amplification factor that depends only on the duration of the trend and the glacier response time, τ. The probability density function (PDF) for s_b is generated by combining the signal-to-noise ratios of the observed melt-season temperature and annual-mean precipitation trends, normalized by the summer (b_s) and winter (b_w) mass-balance variability (Supplementary Fig. 1a,b,c), respectively. We take $\sigma_{b_w} = 0.3\ \mathrm{myr}^{-1}$ and $\sigma_{b_s} = 0.5\ \mathrm{myr}^{-1}$, based on the observed mass-balance variability at Gulkana Glacier and the analysis of the global datasets of glacier mass balance[33]. The glacier response time is given by $\tau = -H/b_t$, where H is a characteristic glacier thickness, and b_t is the (negative) net mass balance at the terminus. We set $H = 590$ m, based on the scaling relationship for glacier geometry suggested by Haeberli and Hoelzle[34] and measured cross-sections[35]; and we set $b_t = -7\ \mathrm{myr}^{-1}$, estimated by extrapolating the vertical mass-balance profiles calculated by Flowers *et al.*[8], thus giving a central estimate for τ of ∼80 years. A PDF is estimated assuming τ follows a gamma distribution incorporating a broad uncertainty of $\sigma_\tau = \tau/4$ (Supplementary Fig. 1d). The PDFs for γ and s_b are combined to give a PDF for σ_L from the relation $\sigma_L = \gamma \Delta L|^{obs} s_b$. This, in turn, is used to evaluate the null hypothesis that $\Delta L|^{obs}$ occurred due to natural variability. Supplementary Fig. 1e shows our estimate that there is only a 0.5% chance that the observed retreat of Kaskawulsh Glacier happened in the absence of a climate trend.

Code availability. The three-stage glacier model code is available from: http://earthweb.ess.washington.edu/roe/GerardWeb/Home.html.

Data availability. The data that support the findings of this study are available from the corresponding author upon request. Publicly available data sources used in this study include the ASTER GDEM v2, available from https://asterweb.jpl.nasa.gov/gdem.asp, Landsat imagery, available from https://landsatlook.usgs.gov, gauge data (Kluane Lake at Burwash Landing,09ca001 and Alsek River, 08ab001) from the Government of Canada, available from https://wateroffice.ec.gc.ca, and meteorological data (Haines Junction, YT) from the Government of Canada, available from http://climate.weather.gc.ca/historical_data/search_historic_data_e.html.

References

30. Carrivick, J. L., Smith, M. W. & Quincey, D. J. *Structure from Motion in the Geosciences* 197 (Wiley Blackwell, 2016).
31. Noh, M.-J. & Howat, I. M. Automated stereo-photogrammetric DEM generation at high latitudes: Surface Extraction with TIN-based Search-space Minimization (SETSM) validation and demonstration over glaciated regions. *GISci. Remote Sens.* **52,** 198–217 (2015).
32. Brooks, A. H. in *Twenty-First Annual Report of the United States Geological Survey to the Secretary of the Interior 1899–1900. Part II- General Geology, Economic Geology, Alaska* (ed. Walcott, D.) 331–392 (US Geological Survey, 1900).
33. Medwedeff, W. G. & Roe, G. H. Trends and variability in the global dataset of glacier mass balance. *Clim. Dynam.* http://dx.doi.org/10.1007/s00382-016-3253-x (2016).
34. Haeberli, W. & Hoelzle, M. Application of inventory data for estimating characteristics of and regional climate-change effects on mountain glaciers: a pilot study with the European Alps. *Ann. Glaciol.* **21,** 206–212 (1995).
35. Clarke, G. K. C. in *Icefield Ranges Research Project, Scientific Results* Vol. 1 (eds Bushnell, V. C. & Ragle, R. H.) 89–106 (American Geographical Society, Arctic Institute of North America, 1969).

nature geoscience

SUPPLEMENTARY INFORMATION

DOI: 10.1038/NGEO2932

In the format provided by the authors and unedited.

River piracy and drainage basin reorganization led by climate-driven glacier retreat

Daniel H. Shugar, John J. Clague, James L. Best, Christian Schoof, Michael J. Willis, Luke Copland and Gerard H. Roe

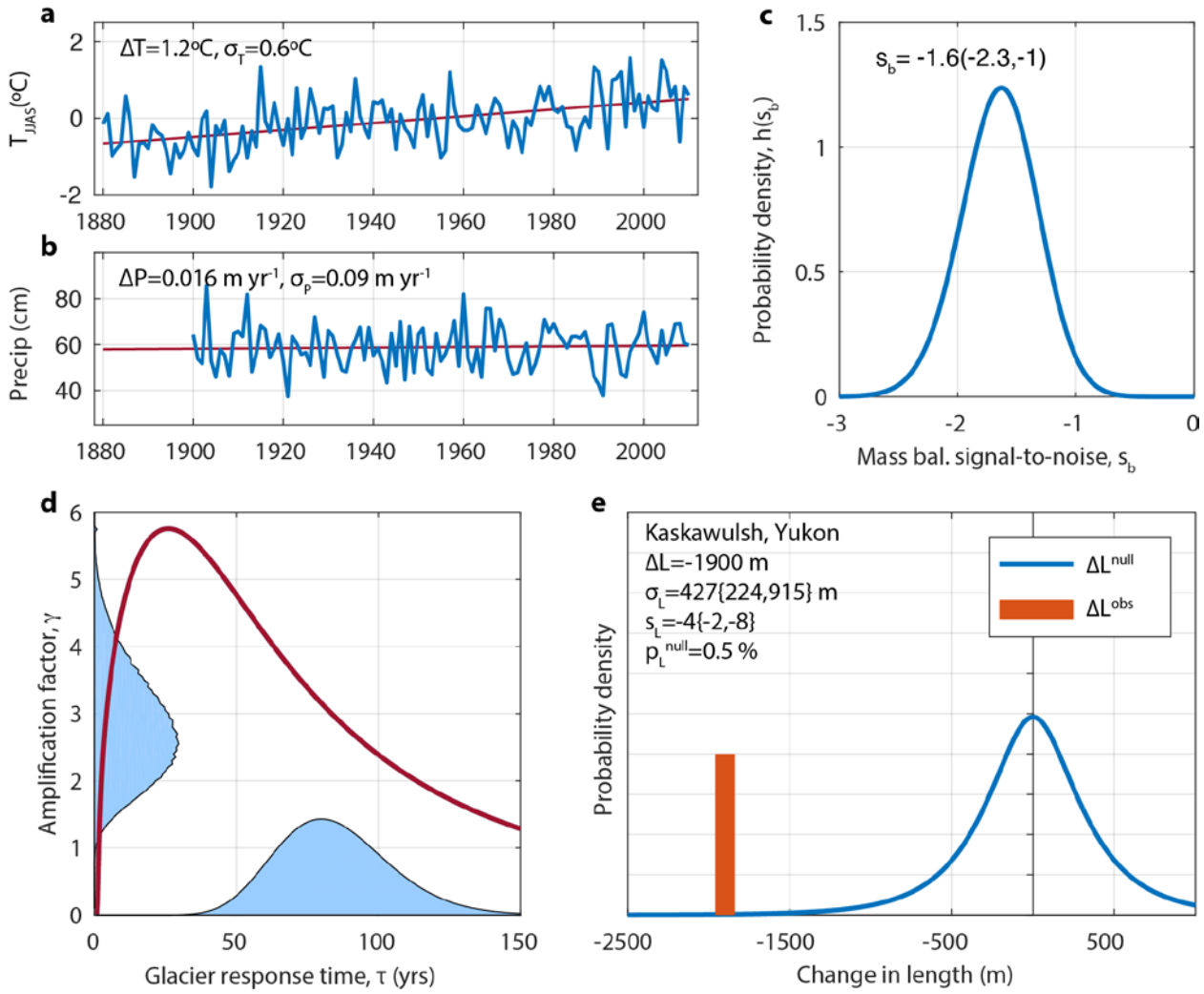

Figure S1. Analysis of climate trends and Kaskawulsh Glacier retreat (1880-2010), following the procedure outlined in Roe et al.[12]. **a**. Melt season surface temperature derived from the Berkeley Earth gridded dataset[1], and least-squares best-fit linear trend. **b**. same as **a**, but for annual mean precipitation obtained from Legates and Wilmott[2] with the trend extrapolated to 1880. **c**. Modeled probability density function (PDF) of the signal-to-noise ratio of mass balance, showing the median and 95% bounds. **d.** Relationship between glacier response time, τ, and the amplification factor, γ, for a 130-yr trend; the red curve shows the relationship between τ and γ; the blue shading on the x-axis shows the PDF for τ and the blue shading on the y axis shows the PDF of γ, that results from τ being projected onto the y axis via the red line. **e**. PDF for the change in length of Kaskawulsh Glacier, ΔL, in any 130-yr period with no climate change, compared with the observed retreat represented by the vertical red bar.

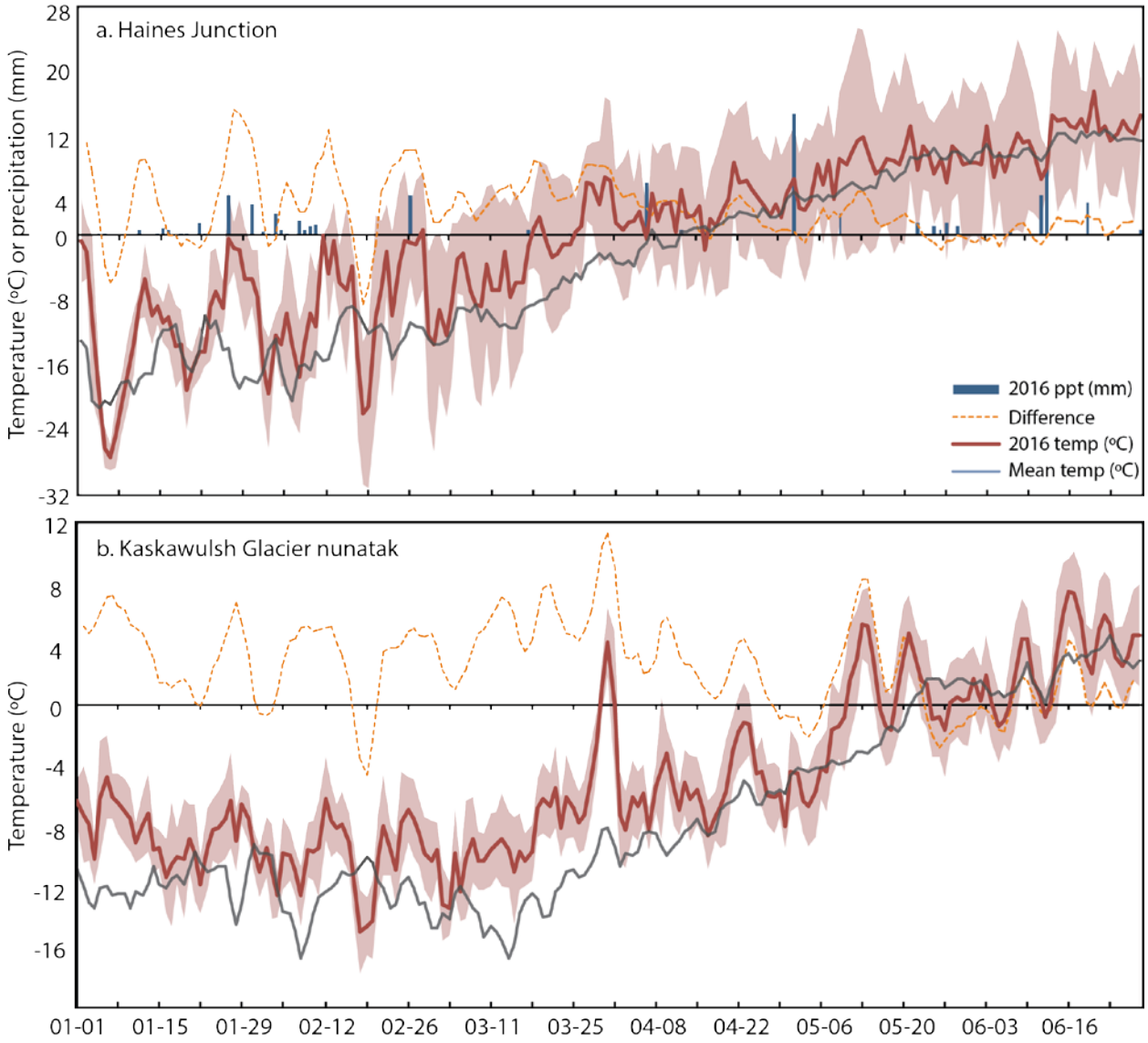

Figure S2. 2016 meteorological measurements from a. Haines Junction (Environment Canada station 2100630) and b. Kaskawulsh Glacier nunatak. At Haines Junction, both precipitation and air temperature are recorded, whereas at the nunatak, only air temperature is recorded. The pink shaded envelope represents the minimum and maximum recorded temperatures for each day in 2016.

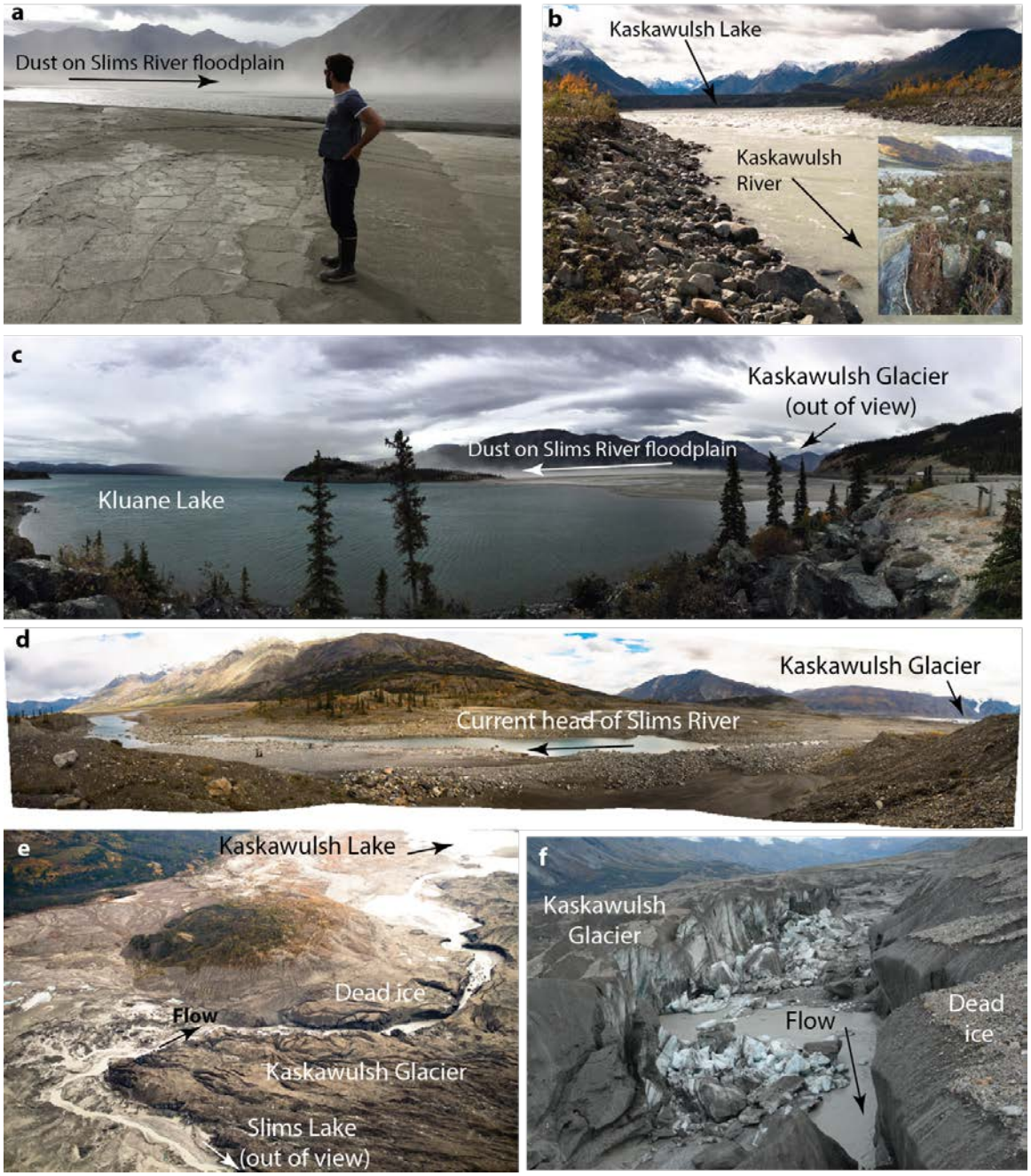

Figure S3. Photos of field area. **a**. Dust storm on Slims River delta with person for scale. **b**. Outlet of Kaskawulsh Lake and Kaskawulsh River with inset of ripped-up root mats caught on boulders and shrub willows. The highest of these root mats was observed 2 m above the river water surface level on September 2, 2016, indicating flood waters were at least that high during peak flows. A flood-deposited sand veneer also covered the banks. **c**. Dust storm on Slims River delta viewed from the north side of Kluane Lake. **d**. Panorama of the current head of Slims River flowing right to left. **e**. Aerial view of the terminus of Kaskawulsh Glacier showing the canyon connecting Slims Lake (out of view at bottom of frame) to Kaskawulsh Lake. Note the presence of dead ice on the downglacier side of the canyon, abutting the hill. **f**. Close-up aerial view of the canyon from described in **e** but facing upstream.

Table S1. List of satellite images used in the analysis.

Sensor	Satellite granule ID	Date of imagery
Landsat-1	LM10670171972246AAA02	09-02-1972
Landsat-2	LM20670171980177PAC00	06-25-1980
Landsat-5	LM50620171990201PAC00	07-20-1990
Landsat-7	LE70620172000189AGS00	07-09-2000
Landsat-7	LE70610182010257EDC00	09-14-2010
Landsat-8	LC80620172015142LGN00	07-25-2015
Landsat-8	LC80610172016170LGN00	06-18-2016
Landsat-8	LC80610172016186LGN00	07-04-2016
SPOT-5	SPOT5_HRG2_XS_20150814_N1_TUILE_SlimsRiver CanadaD0000B0000	08-14-2015
WorldView-1	WV01_20121029_102001001D5D0B00	10-29-2012
WorldView-1	WV01_20121029_102001001E70E600	10-29-2012

Supplementary References

1. Rohde, R., *et al.* A new estimate of the average earth surface land temperature spanning 1753 to 2011. *Geoinfor. Geostat.*, **1**, doi:10.4172/2327-4581.1000101 (2012).

2. Legates, D. R., Willmott, C. J. Mean seasonal and spatial variability in gauge corrected global precipitation. *Intl. J. Clim.*, **10**, 111-127 (1990).